Catalysis Today 178 (2011) 42–46

Contents lists available at ScienceDirect

Catalysis Today

journal homepage: www.elsevier.com/locate/cattod

Whisker carbon in perspective

S. Helveg*, J. Sehested, J.R. Rostrup-Nielsen

Haldor Topsøe A/S, Nymøllevej 55, DK-2800 Kgs. Lyngby, Denmark

ARTICLE INFO

Article history:
Received 12 April 2011
Received in revised form 29 June 2011
Accepted 30 June 2011
Available online 6 August 2011

Keywords:
Whisker carbon
Nickel catalysts
Steam reforming
Electron microscopy

ABSTRACT

A summary is given of the work that aims at describing the parameters guiding the formation of whisker carbon as well as at understanding the growth mechanism. David Trimm played an important role in the pioneering work. The present knowledge is illustrated by recent high-resolution electron micrographs.

1. Introduction

Whisker carbon is formed as characteristic fibers by dissociation of CO, CH_4 and higher hydrocarbons over metal particles [1,2]. The "whisker" typically grows as a carbon fiber with a metal crystal at the top as shown in Fig. 1. Whisker carbon is an important phenomenon in the process industry. The whisker has high strength and destroys the catalyst particle when it hits the pore wall. In a tubular reformer broken catalyst pellets and carbon may have a serious impact on the operation of the reformer by maldistribution of feed and overheating of the tubes [1]. Whisker carbon may also be formed in other processes (high temperature methanation for synthetic natural gas [3], Fischer–Tropsch synthesis [4]) and be involved in coking of tube walls in steam crackers [5] and in nucleation of metal dusting corrosion [1,6]. The so-called carbon nanotubes and other carbon-based nanofiber structures are also considered for a variety of nanotechnological applications including the use as catalyst support [2,7–9]. This paper addresses the formation of whisker carbon on metal catalysts with the intend to inhibit the process.

2. Empirical evidence

2.1. Morphology

For the whisker carbon, different degree of graphitization and morphologies of the graphene layers may be encountered [7,10]. The specific conformation of the graphene layers couples to the metal particle shape, which can adopt e.g. a pear-like shape, and often small fragments of the metal are left behind in the whisker as shown in Fig. 1. The whisker structures are also closely related to those of the carbon nanotubes [7,10,11].

The whisker structure was observed early [12] by examination in an electron microscope. Later studies by Baker et al. [13,14] indicated the whiskers to be hollow as also confirmed recently by high-resolution transmission electron microscopy (HRTEM), as in Fig. 1b. Other early studies by Gwathmey and Cunningham [15] showed a preference for carbon deposition on the on Ni (1 1 1) surface and Grenga and Lawless [16] showed that the nucleation was preferred on kinks and steps.

The importance of step sites (B5 sites) was also indicated by TGA studies [17] and confirmed by later in situ HRTEM observations and density functional theory (DFT) calculations [10,18] (Fig. 2). These studies [10] also demonstrated that the process of carbon deposition is very dynamic involving drastic changes of the shape of the nickel crystal during the nucleation.

Baker and Sherwood [19] demonstrated by means of in situ electron microscopy that the growth mechanism could be reversed with nickel crystals "eating" their way through the carbon leaving channels behind them.

The growth mechanism appears to be the same, irrespective of the type of hydrocarbon or of whether it results from the endothermic dissociation of methane or the exothermic dissociation of carbon monoxide [20]. However, the resulting morphology and degree of graphitisation depend on parameters such as type of hydrocarbon, metal, particle size and temperature. Hence, there might not be a unique growth mechanism for the formation of carbon fibers and nanotubes [7,11].

* Corresponding author.
E-mail address: sth@topsoe.dk (S. Helveg).

0920-5861/$ – see front matter © 2011 Elsevier B.V. All rights reserved.
doi:10.1016/j.cattod.2011.06.023

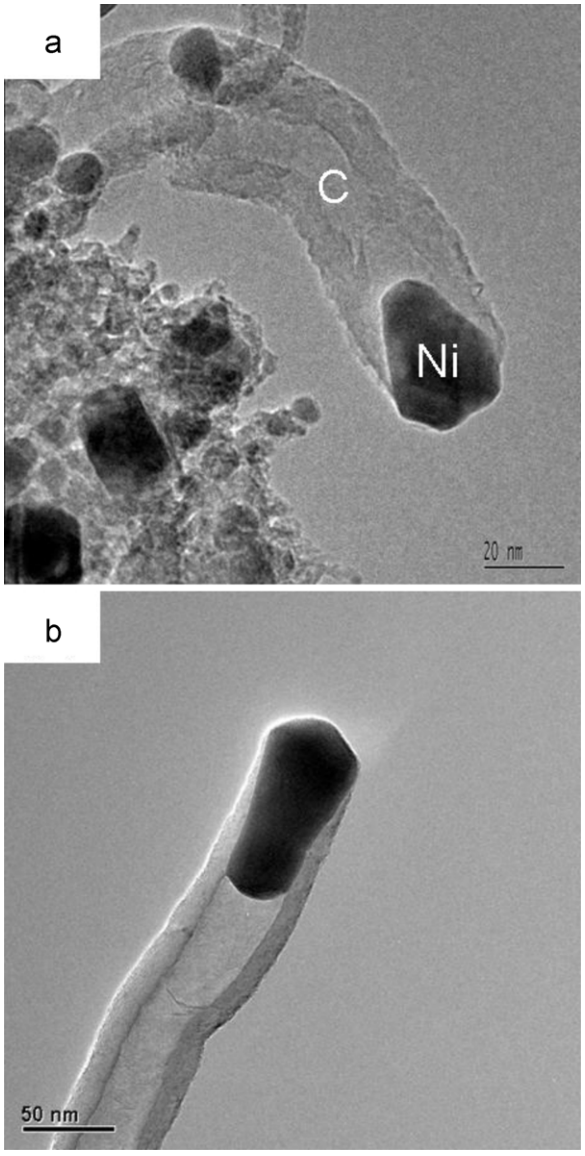

Fig. 1. (a and b) HRTEM images of carbon whiskers.

Whisker carbon is not the only type of carbon formed on nickel catalysts. Depending on the process conditions carbon may be deposited as graphitic layers [1,21,22] which encapsulate the nickel particle as illustrated in Fig. 3.

Whisker carbon is also observed on cobalt and iron catalysts [11,23,24] and the rate of carbon deposition was found to be far less on noble metals than on nickel [23,25]. Carbon deposited on the noble metals was observed to be of a structure that was difficult to distinguish from the catalyst structure [25]. On a ruthenium catalyst, HRTEM revealed a structure which looked like a few atomic layers of carbon covering most of the surface (Fig. 4).

The nickel particle size has an impact on the nucleation of carbon. The smaller the crystals, the more the initiation of carbon nucleation is impeded [1,20]. The whisker growth mechanism is blocked by sulfur poisoning of the nickel surface. When deposited in the presence of sulfur, the carbon has a typical "octopus" structure with several fibers growing from one metal crystal [26]. A similar structure is formed on Ni/Cu catalysts with high copper contents [27].

Fig. 5 shows an example of several fibers growing from one metal particle. Carneiro et al. [11] demonstrated that the fiber growth can be strongly influenced on bimetal particles.

2.2. Rates and equilibria

The rate of carbon formation depends strongly on the type of hydrocarbon with alkenes (and acetylene) being the most reactive [17]. After an induction time, t_0, the carbon grows at a constant rate

$$\frac{dC_w}{dt} = k_c(t - t_0) \quad (1)$$

as shown by thermogravimetric analysis (TGA) measurements [17,21]. This is in contrast to the carbon formation on acidic catalysts on which the coking rate decreases with time as a result of deactivation of the sites for carbon formation and typically expressed by the Vorhies equation [28].

Olefins and acetylene show rapid dissociation and the diffusion of carbon through nickel has been suggested for the rate determining step [13] which is in line with the activation energy for carbon formation being close to that for the diffusion of carbon through nickel. TGA studies by Trimm et al. [21,23,29–31] on carbon formation from olefins showed a complex rate dependency with temperature with an optimum typically around 550–650 °C. At high

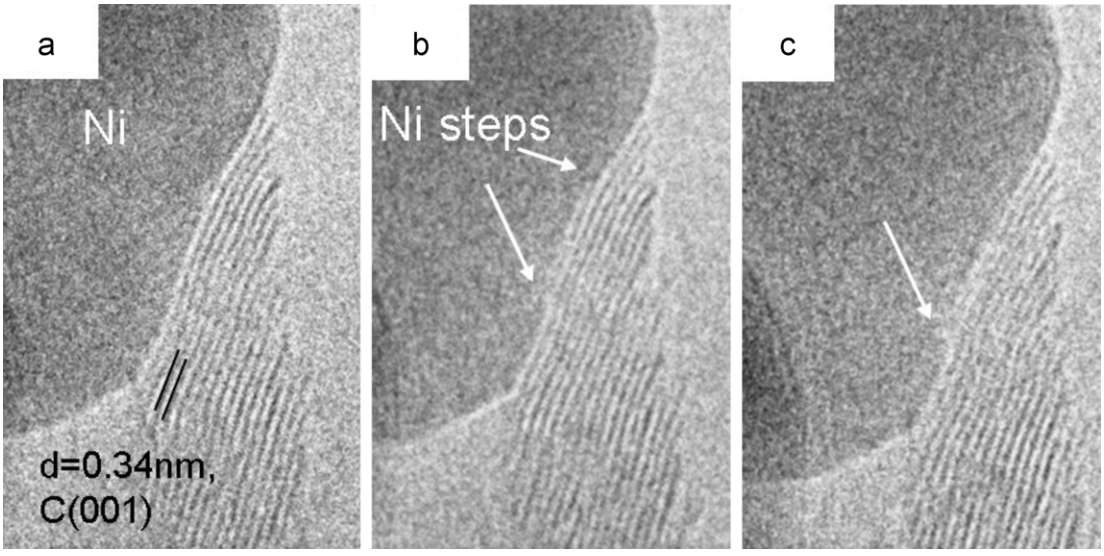

Fig. 2. Time-lapsed HRTEM image series at the whisker–Ni interface acquired in situ during whisker growth. The images reveal that mono-atomic step-edges form spontaneously and assist the growth of additional graphene layers at the interface. Extracted from movie in [10].

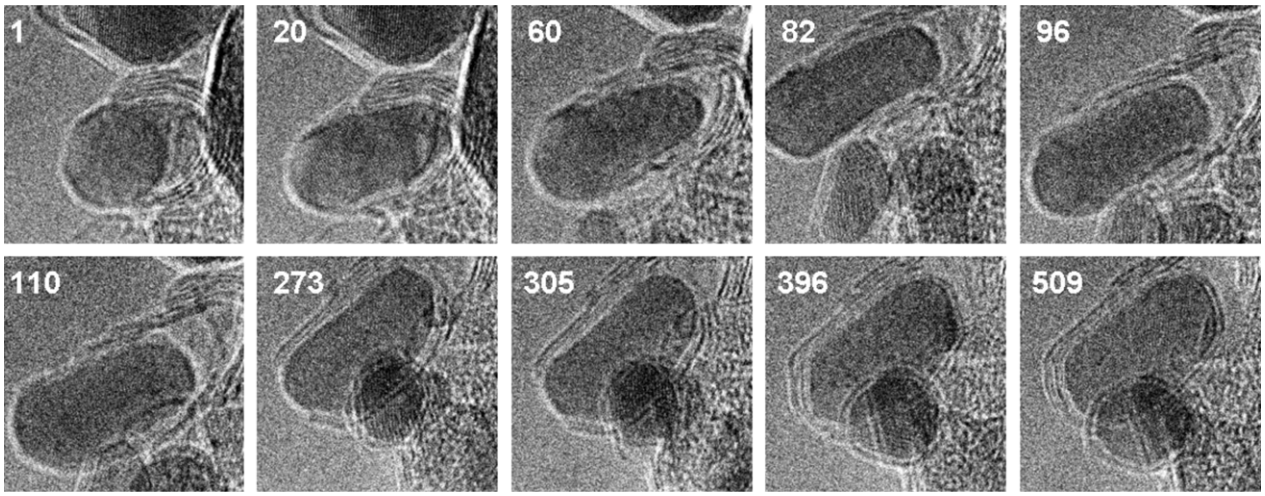

Fig. 3. Snapshots from an in situ HRTEM movie showing growth of multiple graphene layers and the competition between shape dynamics and graphite encapsulation of a Ni nanoparticle. The relative time in seconds are given in the images. The movie was acquired by exposing a nickel catalyst to a 1:1 mixture of hydrogen and methane at a total pressure of 2 mbar at 540 °C.

temperatures the reaction is overlapped by pyrolysis resulting in coke deposits encapsulating the catalyst. This was also reflected by hysteresis phenomena [31,32]. Similar temperature optimum was observed in TGA studies at conditions for steam reforming of heptane [17].

The addition of potassium results in a significant increase in the induction time for methane decomposition [1]. This implies a retarding role of potassium on the dissociation of methane and the nucleation of carbon. Other TGA studies at steam reforming conditions confirmed the promoting role of alkali and of a number of oxides (MgO, La_2O_3, CeO_2) and other components (Bi, Sn) [1,33].

The formation of whisker carbon cannot be tolerated in a tubular reformer [1]. The important question is whether or not carbon is formed, and not the rate at which it may be formed. In terms of the growth mechanism, it means to extend the induction period (t_0 in Eq. (1)) to infinity. The carbon formation depends on the kinetic balance between the surface reaction of the adsorbed hydrocarbon with oxygen species and the further dissociation of the hydrocarbon into adsorbed carbon atoms, which can nucleate to whisker carbon. The decomposition reactions of methane and carbon monoxide are reversible and the risk of carbon formation can be determined by thermodynamics. One may apply the principle of equilibrated gas [1] stating: carbon formation is to be expected on a nickel catalyst if the gas shows affinity for carbon after the establishment of the methane reforming and the shift equilibrium.

The whisker carbon has a higher energy than graphite, which is reflected in lower equilibrium constants for the reversible decomposition reactions of carbon monoxide (the Boudouard reaction) and of methane [20,27,34,35]. This was reported already in 1929 by Dent and Cobb [34]. It was found [20] that the deviation from graphite thermodynamics depends on the nickel particle size and that the deviation could be explained by the extra energy required by the higher surface energy, the elastic energy, and defect struc-

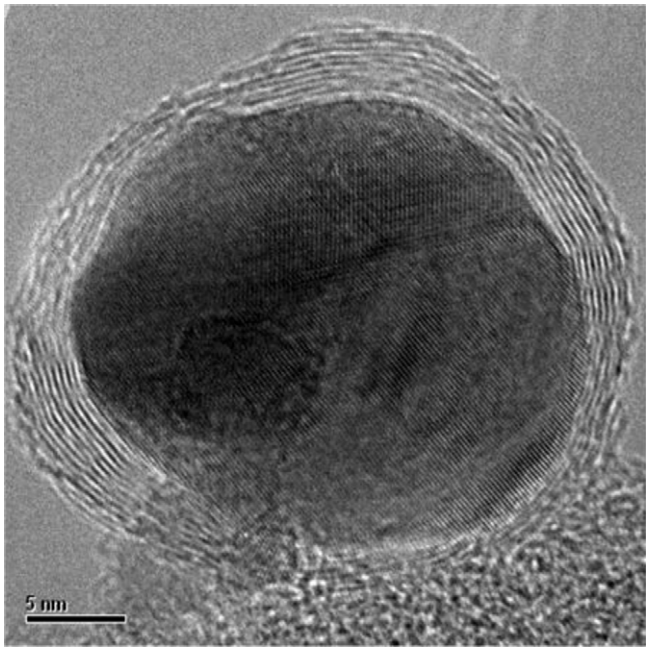

Fig. 4. HRTEM image showing multiple graphene layers encapsulating a Ru nanoparticle.

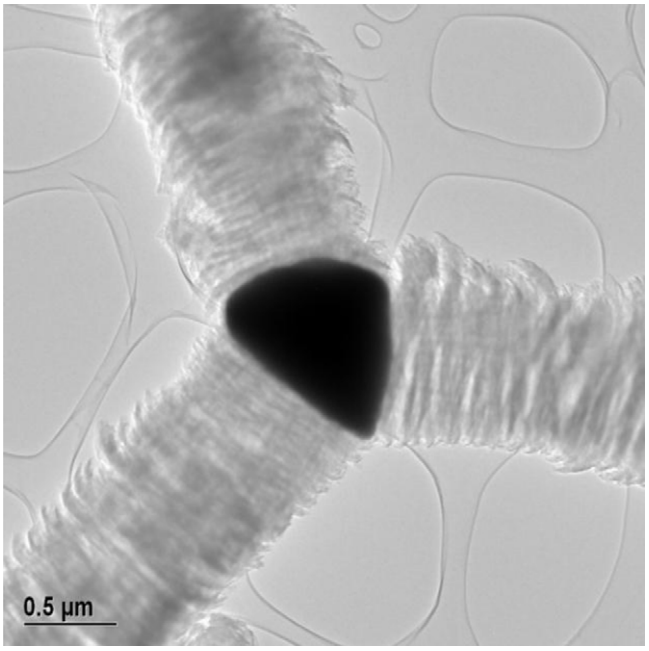

Fig. 5. TEM image of an "octopus"-type carbon structure.

ture of the carbon filaments. Attempts to explain the deviation from graphite data by means of "intermediate carbides" are misleading [24,36] as they may not impact the overall equilibrium constant. Nickel carbide is not stable under steam reforming conditions.

The noble metals have even smaller equilibrium constants for carbon formation [25]. This is due to the metal particle size effect and to other structural effects. Palladium shows a different behavior than the other metals, probably due to the formation of an interstitial solid solution and mobility of carbon in palladium [37].

3. Mechanism

3.1. Classical mechanism

Baker et al. [13] proposed a mechanism for the whisker carbon growth by assuming that the diffusion process of carbon from the free nickel surface through the nickel to the growth center is governed by the temperature gradient resulting from the exothermic decomposition of acetylene. It was justified by the finding that the activation energy for the whisker growth is close to that for diffusion of carbon in nickel (adjusted for the heat of solution of carbon in nickel). Although this might work for the exothermic decomposition of CO, the explanation does not hold for whisker growth by the endothermic decomposition of methane. This apparent contradiction led Trimm and Rostrup-Nielsen [32] to propose an alternative growth mechanism in which the carbon transport was driven by concentration gradients. Specifically, it was suggested that carbon atoms diffuses through the metal particle and nucleates into the fiber at the rear interface at sites favorable for graphene nucleation. Both explanations are based on bulk diffusion of carbon being dissolved in nickel and could explain the low reactivity on noble metals [23] as these do not dissolve carbon.

3.2. New approach

The mechanism of formation of whisker carbon is better understood on the basis of recent studies, including DFT calculations [18,38], adsorption studies [39], and observations by in situ HRTEM [10], which focus on the role of the metal surface in the nucleation and growth of the graphene layers. There is strong evidence for the importance of atomic step sites in the mechanism for carbon formation over nickel. Early indications of the importance of surface heterogenity for carbon formation were obtained by measurements on single metal crystals [15,16]. More recently it was directly observed by HRTEM how the graphene layers grow from surface steps, which are created during the carbon nucleation and moves as the graphene layers grow. Subsequent HRTEM studies showed similarly that surface steps act as growth centers for graphene on Ni and Fe [40–42]. Even for single-crystalline Ru surfaces, steps were reported as graphene growth centers [43–45].

The role of step sites was explained by DFT calculations [18,38,39]. These calculations also indicated that the "classic" mechanism is a simplification. Step sites have a lower activation barrier for all the reaction steps in the dehydrogenation of methane and all the intermediates are more strongly bound than on the close-packed nickel surfaces. However, activation of methane is possible also at terrace sites of nickel as opposed to CO [39,46,47]. However, carbon is bound much stronger on the step sites than on the flat surface, suggesting that the nucleation of graphene layers preferentially occurs at step sites [18,38,39]. Furthermore, the carbon atoms are bound stronger in a graphene layer than to the step sites, thus creating a driving force for the graphene growth from the step sites. This is the case for sufficiently large graphene islands but for smaller graphene islands, the excess energy of the graphene edge will dominate over the bulk energy gain of carbon

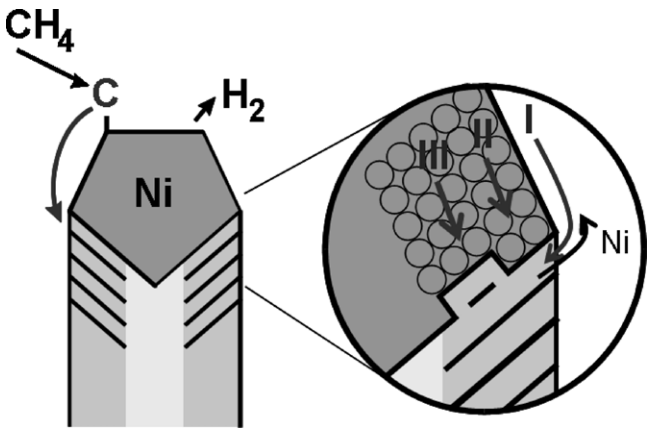

Fig. 6. Illustration of the whisker growth mechanism based on step-site mediated graphene growth and transport processes confined to the surface region, as discussed in Ref. [18].

in the graphene layer and increase the total energy to be above the energy of a carbon atom at a step edge. Graphene islands below a critical size will thus tend to decrease and disappear while islands above a critical size will increase in size and eventually lead to formation of a large sheet of graphene. A finite size of the critical island size is also consistent with the observation that carbon is not formed on catalysts with small nickel crystals because the size of the critical graphene sheet is larger then the atomic planes at the metal particles [38,48].

The HRTEM observations clearly pointed to a surface transport of the metal atoms from the step sites to the free metal surface (Fig. 6), and although there is a transport of carbon atoms from the adsorption site on the free surface to the growth center, the carbon transport was not resolved in the HRTEM images. However, the DFT calculations could examine the different diffusion paths of carbon along the metal nanoparticles. It was shown that the largest barrier is associated with the carbon transport [10,18] and it was concluded that diffusion through the bulk phase is very unlikely as compared to surface diffusion [18,49]. Specifically, Abild-Pedersen et al. [18] calculated that bulk transport through a Ni crystal is associated with an activation energy of about 225 kJ/mol, which is about 100 kJ/mol more than for transport paths involving surface diffusion and perhaps diffusion through the sub-surface layer of nickel. The preference for the surface and sub-surface paths was related to lattice relaxations, which are possible in the surface but prohibited in the bulk metal [18]. The picture that emerges is clearly in contrast to the mechanisms based on bulk diffusion of carbon, whether based on assumptions of temperature gradients [13] or of concentration gradients [32]. The discrepancy is likely structural in origin; the activation barrier for carbon diffusion was originally measured using polycrystalline nickel foils and defects or grain boundaries on such films are possibly responsible for the faster measured C bulk diffusion than that calculated by DFT on single-crystals, as pointed out in [18].

The difficulty in carbon formation on most noble metals has traditionally been explained by the lack of bulk diffusion of carbon in these metals due to low solubility of carbon in these metals. However, even though the bulk metal may contribute to growth, the surface processes seem to be sufficient to explain graphene growth from gaseous precursors over different metals [48,50]. An important factor is that the bond strength of carbon to the metals [51], which determines whether the coverages of carbon is sufficient for the nucleation of graphene. Recent studies of the new step-flow growth model offers a more complete picture for graphene growth over different transition metals. From a series of DFT calculations of carbon adsorption energies, it was argued that graphene grows

preferentially out from surface step edges onto lower facets on fcc and hcp metal surfaces [48]. Moreover, a simple model for the critical graphene nucleus size was proposed in which the critical size is influenced by the energy cost for the graphene edge and, surprisingly, an epitaxial lattice match between graphene and the metal step-edge as well as the carbon chemical potential for graphene formation. The simple model allowed for a description of observed trends in graphene formation for different transition metal surfaces under varying experimental conditions.

The finding that step sites act as preferential growth centers for graphene has allowed for a more general understanding of many different promoters in Ni-based reforming catalysts to be developed: DFT calculations [38,39] have shown that a number of different ad-atoms including potassium, sulfur and gold [38,39] also bind preferentially to step sites suggesting that the promotional effect involves the blockage of step sites for nucleation of carbon. The blockage of sites for carbon nucleation was the idea of the SPARG process [26] with chemisorbed sulfur "passivating the ensembles" for nucleation of carbon. An alternative route for engineering the step-site properties could also involve alloying [52,53].

4. Conclusions

The mechanism of formation of whisker carbon has been the subject of a continuous effort over several decades with early work by represented by Dent, Gwatmey and others followed by in situ electron microscopy by Baker et al., Geus et al. and TGA work by Trimm et al. and the Topsoe group. The main findings on the role of step sites have been confirmed by recent efforts by means of well defined adsorption studies and in situ HTREM combined with DFT calculations by the Nørskov team. This has lead to a better understanding of the mechanism and means for promotion for carbon free operation.

References

[1] J.R. Rostrup-Nielsen, L.J. Christiansen, Concepts in Syngas Manufacture, Imperial College Press, London, 2011.
[2] M.K. van der Lee, A.J. van Dillen, J.W. Geus, K.P. de Jong, J.H. Bitter, Carbon 44 (2006) 629.
[3] J.R. Rostrup-Nielsen, in: J.L. Figueiredo (Ed.), Progress in Catalyst Deactivation, Martinus Nijhof, The Hague, 1982, p. 127.
[4] E. Iglesia, S.L. Soled, R.A. Fiato, G.H. Via, J. Catal. 143 (1993) 345.
[5] D.L. Trimm, in: L.F. Albright, B.L. Crynes, W.H. Corocan (Eds.), Pyrolysis: Theory and Industrial Practice, Academic Press, New York, 1983, p. 203, chapter 9.
[6] Z. Zeng, K. Natesan, Chem. Mater. 17 (2005) 3794.
[7] K. de Jong, J.W. Geus, Catal. Rev. - Sci. Eng. 42 (2000) 481.
[8] R.H. Baughman, A.A. Zakhidov, W.A. de Heer, Science 297 (2002) 787.
[9] J.M. Schnorr, T.M. Swager, Chem. Mater. 23 (2011) 646.
[10] S. Helveg, C. López-Cartes, J. Sehested, P.L. Hansen, B.S. Clausen, J.R. Rostrup-Nielsen, F. Abild-Pedersen, J.K. Nørskov, Nature 427 (2004) 426.
[11] O.C. Carneiro, N.M. Rodriguez, R.T.K. Baker, Carbon 43 (2005) 2398.
[12] L.J.E. Hofer, E. Sterling, J.T. McCartney, J. Phys. Chem. 59 (1955) 1153.
[13] R.T.K. Baker, M.A. Barber, F.S. Feates, P.S. Harris, R.J. Waite, J. Catal. 26 (1972) 51.
[14] R.T.K. Baker, M.A. Baber, P.S. Harris, T.B. Thomas, R.J. Waite, J. Catal. 30 (1973) 86.
[15] A.T. Gwathmey,.R.E. Cunningham, Adv. Catal. 10 (1958) 57.
[16] H.E. Grenga, K.R. Lawless, J. Appl. Phys. 43 (1972) 1508.
[17] J.R. Rostrup-Nielsen, J. Catal. 33 (1974) 184.
[18] F. Abild-Pedersen, J.K. Nørskov, J.R. Rostrup-Nielsen, J. Sehested, S. Helveg, Phys. Rev. B73 (11) (2006) 115419.
[19] R.T.K. Baker, R.D. Sherwood, J. Catal. 70 (1981) 198.
[20] J.R. Rostrup-Nielsen, J. Catal. 27 (1972) 343.
[21] L.S. Lobo, D.L. Trimm, J. Catal. 29 (1973) 15.
[22] G.H. Renshaw, C. Roscoe, P.L. Walker Jr, J. Catal. 22 (1971) 394.
[23] L.S. Lobo, D.L. Trimm, J.L. Figueiredo, Proc. 5th. Int. Congr. Catal., Palm Beach 1972, Elsevier, Amsterdam, 1973, vol. 2, p. 1125.
[24] A.J.H.M. Koch, P.K. de Bokx, E. Boellard, W. Klop, J.W. Geus, J. Catal. 96 (1985) 468.
[25] J.R. Rostrup-Nielsen, J.-H. Bak Hansen, J. Catal. 144 (1993) 38.
[26] J.R. Rostrup-Nielsen, J. Catal. 85 (1984) 31.
[27] C.A. Bernardo, I. Alstrup, J.R. Rostrup-Nielsen, J. Catal. 96 (1985) 517.
[28] Vorhies Jr., Ind. Eng. Chem. 37 (1945) 318.
[29] D.L. Trimm, Catal. Rev. - Sci. Eng. 16 (1977) 155.
[30] F.J. Derbyshire, D.L. Trimm, Carbon 13 (1975) 189.
[31] J.L. Figueiredo, D.L. Trimm, Proc. 4th London Inc. Carbon and Graphite Conference, Society for Chemical Industry, London, 1974, p. 314.
[32] J.R. Rostrup-Nielsen, D.L. Trimm, J. Catal. 48 (1977) 155.
[33] D.L. Trimm, Catal. Today 37 (1997) 233.
[34] F.J. Dent, J.W. Cobb, J. Chem. Soc. 2 (1929) 1903.
[35] F.J. Dent, L.A. Moignard, A.H. Eastwood, W.H. Blackburn, D. Hebden, Trans. Inst. Gas Eng. (1945–46) 602.
[36] T. Nicklin, R.J. Whittaker, Inst. Gas Eng. J. 8 (1968) 15.
[37] S.B. Ziemecki, Stud. Surf. Sci. Catal. 38 (1987) 625.
[38] H.S. Bengaard, J.K. Nørskov, J. Sehested, B.S. Clausen, L.P. Nielsen, A.M. Molenbroek, J.R. Rostrup-Nielsen, J. Catal. 209 (2002) 365.
[39] J.R. Rostrup-Nielsen, J. Sehested, J.K. Nørskov, Adv. Catal. 47 (2002) 65.
[40] S. Hofmann, R. Sharma, C. Ducati, G. Du, C. Mattevi, C. Cepek, M. Cantoro, S. Pisana, A. Parvez, F. Cervantes-Sodi, A.C. Ferrari, R. Dunin-Borkowski, S. Lizzit, L. Petaccia, A. Goldoni, J. Robertson, Nanoletters 7 (2007) 602.
[41] J.A. Rodríguez-Manzo, M. Terrones, H. Terrones, H.W. Kroto, L. Lun, F. Banhart, Nat. Nano 2 (2007) 307.
[42] M. Lin, J.P.Y. Tan, C. Boothroyd, K.P. Loh, E.S. Tok, Y.-L. Foo, Nanoletters 7 (2007) 2234.
[43] M.-C. Wu, Q. Xu, D.W. Goodmann, J. Phys. Chem. 98 (1994) 5104.
[44] S. Marchini, S. Günther, J. Wintterlin, Phys. Rev. B 76 (2007) 075429.
[45] P.W. Sutter, J.-I. Flege, E.A. Sutter, Nat. Mater. 7 (2008) 406.
[46] R.A. van Santen, M. Neurock, S.G. Shelly, Chem. Rev. 110 (2010) 2005.
[47] G. Jones, J.G. Jakobsen, S.S. Shim, J. Kleis, M.P. Anderson, J. Rossmeisl, F. Abild-Pedersen, T. Bligaard, S. Helveg, B. Hinnemann, J.R. Rostrup-Nielsen, I. Chorkendorff, J. Sehested, J.K. Nørskov, J. Catal. 259 (2008) 147.
[48] S. Saadi, F. Abild-Pedersen, S. Helveg, J. Sehested, B. Hinnemann, C.C. Appel, J.K. Nørskov, J. Phys. Chem. C 114 (2010) 11221.
[49] S. Hofmann, G. Csányi, A.C. Ferrari, M.C. Payne, J. Robertson, Phys. Rev. Lett. 95 (2005) 036101.
[50] O.V. Yazyev, A. Pasquarello, Phys Rev. Lett. 100 (2008) 156102.
[51] T. Bligaard, J.K. Nørskov, S. Dahl, J. Mathiesen, C.H. Christensen, J. Sehested, J. Catal. 224 (2004) 206.
[52] S. Saadi, B. Hinnemann, S. Helveg, C.C. Appel, F. Abild-Pedersen, J.K. Nørskov, Surf. Sci. 603 (2009) 726;
S. Saadi, B. Hinnemann, S. Helveg, C.C. Appel, F. Abild-Pedersen, J.K. Nørskov, Ibid 605 (2011) 582.
[53] E. Nikolla, A. Holewinski, J. Schwank, S. Linic, J. Am. Chem. Soc. 128 (2006) 11354.